Bioorganic Chemistry 90 (2019) 103063

Contents lists available at ScienceDirect

Bioorganic Chemistry

journal homepage: www.elsevier.com/locate/bioorg

Synthesis, molecular docking and kinetic studies of novel quinolinyl based acyl thioureas as mushroom tyrosinase inhibitors and free radical scavengers

Muhammad Naeem Mustafa[a], Aamer Saeed[a,*], Pervaiz Ali Channar[a], Fayaz Ali Larik[a], Muhammad Zain-ul abideen[a], Ghulam Shabir[a], Qamar Abbas[c], Mubashir Hassan[b], Hussain Raza[b], Sung-Yum Seo[b]

[a] Department of Chemistry, Quaid-I-Azam University, Islamabad 45320, Pakistan
[b] Department of Biological Sciences, College of Natural Sciences, Kongju National University, 56 Gongjudehak-Ro, Gongju, Chungnam 314-701, Republic of Korea
[c] Department of Physiology, University of Sindh, Jamshoro 76080, Pakistan

ARTICLE INFO

Keywords:
Molecular docking
Kinetics
Quinolinyl acyl thioureas
Mushroom tyrosinase inhibitors
Free radical scavengers

ABSTRACT

The enzyme tyrosinase plays a vital role in melanin biosynthesis and enzymatic browning of vegetables and fruits. A series of novel quinolinyl thiourea analogues (**11a-j**) were synthesized by reaction of 3-aminoquinoline and corresponding isothiocyanates, in moderate to excellent yields with different substitutions and their inhibitory effect on mushroom tyrosinase and free radical scavenging activity were evaluated. The compound *N*-(quinolin-3-ylcarbamothioyl)hexanamide (**11c**) exhibited the maximum tyrosinase inhibitory effect (IC_{50} = 0.0070 ± 0.0098 μM) compared to other derivatives and the reference Kojic acid (IC_{50} = 16.8320 ± 0.0621 μM). The docking studies were carried out and the compound (**11c**) showed most negative estimated free energy of −7.2 kcal/mol in mushroom tyrosinase active site. The kinetic analysis revealed that the compound (**11c**) inhibits the enzyme tyrosinase non-competitively to form the complex of enzyme and inhibitor. The results revealed that **11c** could be identified as putative lead compound for the design of efficient tyrosinase inhibitors.

1. Introduction

Acyl thioureas with efficient molecular architecture have made them point of attraction in the scientific community. Acyl thioureas have general functional moiety -OC-NH-CS-NH-. Due to the heteroatomic functionality, acyl thioureas are capable to coordinate to several metal centers as ligands (neutral, monoanionic or dianionic). In addition, heteroatoms (N, O and S) in acyl thioureas have the ability to act as hard or soft electron donor and offer many bonding possibilities for transition metal extraction and ion sensing [1,2]. They play promising role in molecular electronics, material sciences, molecular recognition, pharmaceuticals, agriculture and biological fields.

Acyl thioureas have diverse industrial applications. Colorimetric chemosensors based on acyl thiourea and benzoyl structural elements are used for the detection of copper. They grip the metal atoms through oxygen and sulfur present in acyl thiourea while benzoyl moiety made it visible to naked eye [3]. Acyl thioureas were used as mono- or bidentate ligands to form the ruthenium complexes that exhibit excellent DNA binding properties [4]. Metal complexes with acyl thioureas are efficient source of transition metal sulfides. Transition metal sulfides exhibit good material properties with photonic and energy related applications [5]. Acyl thiourea library of compounds exhibit wide array of biological activities such as HIV inhibition **1** [6], inflammatory inhibition, anticonvulsant **2** [7], anticancer **3** [8], antimicrobial **4** [9], urease inhibitory **5** [10], insecticidal **6** [11] and herbicidal **7** [12] shown in Fig. 1. They act as chelating agents, corrosion inhibitors and exhibit antioxidant properties.

The compounds with acyl thiourea moiety exhibited the mushroom tyrosinase inhibition activity [13]. Tyrosinase is copper containing monooxygenase enzyme which is distributed in plants, microorganisms and animals [14]. It drives the hydroxylation reaction of monophenols to *o*-diphenols and oxidation reaction of *ortho*-diphenols to *ortho*-quinones in the plants [15]. These causes the variations of color, flavor and nutritional quality of vegetables. In vertebrates and fungi, tyrosinase enzyme catalyzes conversion of tyrosine into melanin which is a pigment responsible for color of skin and provide the protection against UV light [16]. The abnormal melanin production results in serious aesthetic concerns in human beings such as hypermelanogenesis, melasma and

* Corresponding author.
E-mail address: asaeed@qau.edu.pk (A. Saeed).

https://doi.org/10.1016/j.bioorg.2019.103063
Received 27 January 2019; Received in revised form 8 June 2019; Accepted 9 June 2019
Available online 12 June 2019

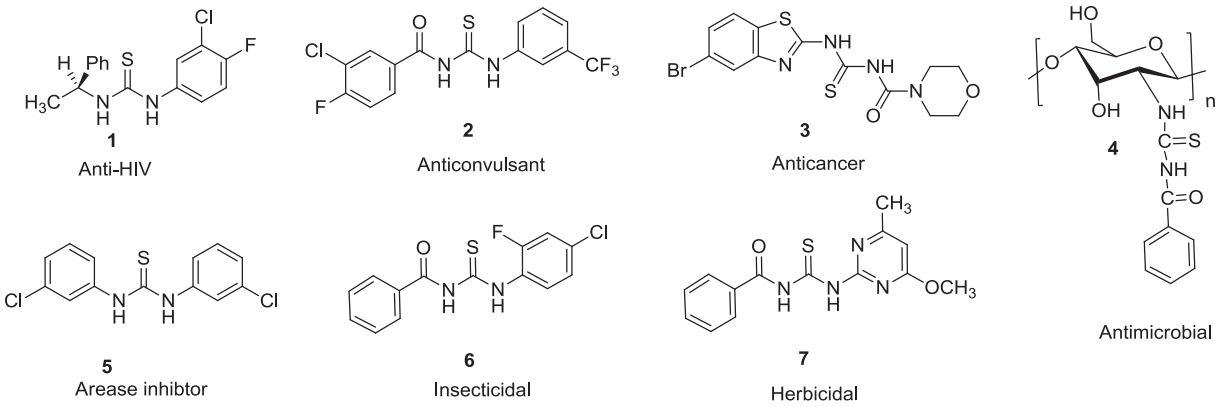

Fig. 1. Structures of biologically active acyl thioureas.

ephelide etc [17]. These studies encouraged many researchers to develop the potent inhibitors of tyrosinase for the utilization in foods and cosmetics.

Quinoline is nitrogen containing aromatic heterocyclic compound and has been displaying expansive spectrum of biological applications such as analgesic, anti-bacterial, anticonvulsant, anthelmintic, anti-fungal, antimalarial, anti-inflammatory and cardiotonic activities [18,19]. Inspired by the importance of quinoline and acyl thiourea functionality we have designed and synthesized the quinoline based acyl thioureas to be utilized as efficient tyrosinase inhibitors.

2. Experimental

2.1. General methods and materials

The R_f-values of the compounds were determined by using aluminum pre-coated silica gel plates Kiesel 60 F_{254} bought from Merck. Gallenkamp melting point apparatus (MP-D) was used to determine the melting points through open capillary method. IR analysis was performed by Bruker FT-IR Bio-Rad-Excalibur Series Mode No. FTS 300 MX spectrometer. The ^{1}H NMR and ^{13}C NMR spectra were recorded on Bruker 300 MHz NMR spectrometer in deuterated DMSO and $CDCl_3$ solutions with tetramethylsilane (TMS) as an internal reference. HPLC-MS analysis was achieved by LC system Agilent 1200 series and the elemental analyses were conducted using a LECO-183 CHNS analyzer.

2.2. General procedure for the synthesis of 11 (*a-j*)

Quinoline based acyl thioureas **11** (**a-j**) were efficiently prepared in moderate to excellent yields. A round bottom flask charged with KSCN (2.08 mmol) and dry acetone (10 ml) was allowed to stand at room temperature with stirring for 5 min followed by the dropwise addition of the equimolar acid chloride solution **8** to yield isothiocyanate **9**. The reaction mixture was refluxed for 2 h and cooled to room temperature. The solution of 3-aminoquinoline **10** (2.08 mmol) was added dropwise with stirring and reaction mixture refluxed for 12 h to furnish quinoline based acyl thioureas **11** (**a-j**). On the completion of reaction, monitored by TLC, mixture was cooled and added to ice cold water to afford precipitates. The precipitates were filtered and purified by recrystallization in ethanol to obtain acyl thioureas **11** (**a-j**).

2.2.1. N-(Quinolin-3-ylcarbamothioyl)butyramide (*11a*)

Light yellow powder (85%); m.p; 183–184 °C; R_f; 0.72 (ethyl acetate:*n*-hexane, 3:7); FT-IR (ATR) in cm^{-1}; 3175 (N—H), 2953, 2870 (H—C, alkyl asym and sym),1686 (C═O), 1591 (C═N), 1537, 1463 (C═C), 1169 (C═S); ^{1}H NMR (300 MHz, $CDCl_3$); δ, 12.80 (s, 1H, NH), 9.37 (s, 1H, NH), 9.21 (s, 1H, ArH), 8.80 (d, 1H, J = 2.1 Hz, ArH), 8.30 (d, 1H, J = 8.1 Hz, ArH), 7.91 (d, 1H, J = 8.4 Hz, ArH), 7.80 (m, 1H, ArH), 7.66 (m,1H, ArH), 2.51 (t, 2H, J = 7.5 Hz, CH_2), 1.80 (sex, 2H, J = 7.5 Hz, CH_2), 1.06 (t, 3H, J = 7.5 Hz, CH_3); ^{13}C NMR (75 MHz, $CDCl_3$); δ, 179.4 (C═O), 174.8 (C═S), 147.3 (C-2, quinolinyl), 146.2, 131.2, 130.5, 129.5, 129.2, 128.1, 128.0, 127.8 (quinolinyl-C), 39.1, 18.2, 13.5 (alkyl-C); HPLC-MS, (*m/z*), 274 [M + H] +, Anal. Calcd. for $C_{14}H_{15}N_3OS$: C, 61.51; H, 5.53; N, 15.37; Found: C, 61.48; H, 5.51; N, 15.34.

2.2.2. N-(Quinolin-3-ylcarbamothioyl)pentanamide (*11b*)

Off-white powder (86%); m.p; 119–120 °C; R_f; 0.55 (ethyl acetate:*n*-hexane, 2:8); FTIR (ATR) in cm^{-1}; 3202 (N—H), 2957, 2870 (H—C, alkyl asym and sym), 1696 (C═O), 1669 (C═N), 1518, 1491 (C═C), 1154 (C═S); ^{1}H NMR (300 MHz, $CDCl_3$); δ, 12.65 (s, 1H, NH), 9.28 (s, 1H, NH), 8.98 (d, 1H, J = 2.1 Hz, ArH), 8.83 (d, 1H, J = 2.1 Hz, ArH), 8.14 (d, 1H, J = 8.1 Hz, ArH), 7.87 (d, 1H, J = 7.8 Hz, ArH), 7.74 (m, 1H, ArH), 7.61 (m,1H, ArH), 2.41 (t, 2H, J = 7.5 Hz, CH_2), 1.53 (m, 4H, alkyl-H), 0.82 (t, 3H, J = 7.2 Hz, CH_3); ^{13}C NMR (75 MHz, $CDCl_3$); δ, 178.3 (C═O), 173.5 (C═S), 147.2 (C-2, quinolinyl), 145.8, 132.1, 130.5, 129.5, 128.8, 128.1, 127.7, 127.2 (quinolinyl-C), 31.4, 24.3, 20.4, 13.8 (alkyl-C); HPLC-MS, (*m/z*), 288 [M + H] +; Anal. Calcd. for $C_{15}H_{17}N_3OS$: C, 62.69; H, 5.96; N, 14.62; Found; C, 62.39; H, 5.92; N, 14.59.

2.2.3. N-(Quinolin-3-ylcarbamothioyl)hexanamide (*11c*)

Off-white powder (86%); m.p; 155–157 °C; R_f; 0.45 (ethyl acetate:*n*-hexane, 3:7); FT-IR (ATR) in cm^{-1}; 3202 (N—H), 2957, 2870 (H—C, alkyl asym and sym), 1696 (C═O), 1669 (C═N), 1518, 1491 (C═C), 1154 (C═S); ^{1}H NMR (300 MHz, $CDCl_3$); δ, 12.74 (s, 1H, NH), 9.36 (s, 1H, NH), 8.96 (d, 1H, J = 2.4 Hz, ArH), 8.79 (d, 1H, J = 2.4 Hz, ArH), 8.12 (d, 1H, J = 8.4 Hz, ArH), 7.85 (dd, 1H, J = 1.2, 8.4 Hz, ArH), 7.73 (m, 1H, ArH), 7.58 (m, 1H, ArH), 2.44 (t, 2H, J = 7.5 Hz, CH_2), 1.73 (m, 2H, CH_2), 1.36 (m, 4H, alkyl-H), 0.92 (t, 3H, J = 7.2 Hz, CH_3); ^{13}C NMR (75 MHz, $CDCl_3$); δ, 179.2 (C═O), 174.8 (C═S), 147.3 (C-2, quinolinyl), 146.3, 131.2, 129.5, 129.1, 128.9, 128.0, 127.5 127.3 (quinolinyl-C), 37.2, 31.1, 24.4, 22.3, 13.8 (alkyl-C); Anal. Calcd. for $C_{16}H_{19}N_3OS$: C, 63.76; H, 6.35; N, 13.94; Found: C, 63.68; H, 6.32; N, 13.89.

2.2.4. N-(Quinolin-3-ylcarbamothioyl)heptanamide (*11d*)

White crystalline (86%); m.p; 104–106 °C; R_f; 0.14 (ethyl acetate:*n*-hexane, 3:7); FT-IR (ATR) in cm^{-1}; 3334 (N—H), 3036 (C—H, Ar), 2917, 2853 (H—C, alkyl asym and sym), 1698 (C═O), 1678 (C═N), 1547, 1492 (C═C), 1186 (C═S); ^{1}H NMR (300 MHz, $CDCl_3$); δ, 12.68 (s, 1H, NH), 9.43 (s, 1H, NH), 8.93 (d, 1H, J = 2.1 Hz, ArH), 8.75 (d, 1H, J = 2.4 Hz, ArH), 8.09 (d, 1H, J = 8.1 Hz, ArH), 7.87 (d, 1H, J = 8.4 Hz, ArH), 7.69 (m, 1H, ArH), 7.55 (m,1H, ArH), 2.38 (t, 2H, J = 7.8 Hz, CH_2), 1.73 (quin, 2H, J = 7.2 Hz, CH_2), 1.33 (m, 6H, alkyl-H), 0.89 (t, 3H, J = 7.5 Hz, CH_3); ^{13}C NMR (75 MHz, $CDCl_3$); δ, 178.5 (C═O), 175.6 (C═S), 148.1 (C-2, quinolinyl), 147.4, 131.5, 129.9, 129.6, 128.7, 128.4, 127.8 127.3 (quinolinyl-C), 36.3, 30.6, 29.7, 25.3,

21.3, 14.7 (alkyl-C); Anal. Calcd. for $C_{17}H_{21}N_3OS$: C, 64.73; H, 6.71; N, 13.32; Found: C, 64.71; H, 6.68; N, 13.30.

*2.2.5. N-(Quinolin-3-ylcarbamothioyl)octanamide (**11e**)*

White crystalline (88%); m.p; 117–119 °C; R_f; 0.62 (ethyl acetate:*n*-hexane, 3:7); FT-IR (ATR) in cm^{-1}; 3181 (N−H), 3031 (C−H, Ar), 2916, 2853 (H−C, alkyl asym and sym), 1692 (C=O), 1620 (C=N), 1532, 1463 (C=C), 1164 (C=S); ^{1}H NMR (300 MHz, acetone-d_6); δ, 12.85 (s, 1H, NH), 10.53 (s, 1H, NH), 9.03 (d, 1H, J = 2.4 Hz, ArH), 8.79 (d, 1H, J = 2.4 Hz, ArH), 8.06 (d, 1H, J = 8.1 Hz, ArH), 7.96 (d, 1H, J = 7.8 Hz, ArH), 7.75 (m, 1H, ArH), 7.62 (m,1H, ArH), 2.62 (t, 2H, J = 7.5 Hz, CH_2), 1.80 (quin, 2H, J = 7.2 Hz, CH_2), 1.34 (m, 8H, alkyl-H), 0.89 (t, 3H, J = 6.6 Hz, CH_3); ^{13}C NMR (75 MHz, acetone-d_6); δ, 180.3 (C=O), 175.5 (C=S), 148.0 (C-2, quinolinyl), 146.1, 132.1, 129.0, 128.4, 128.3, 127.9, 127.6, 127.0 (quinolinyl-C), 36.3, 31.5, 29.7, 28.2, 24.6, 22.4, 13.4 (alkyl-C); Anal. Calcd. for $C_{18}H_{23}N_3OS$: C, 65.62; H, 7.04; N, 12.75; Found: C, 65.58; H, 7.01; N, 12.71.

*2.2.6. N-(Quinolin-3-ylcarbamothioyl)decanamide (**11f**)*

White crystalline (84%); m.p; 120–122 °C; R_f; 0.42 (ethyl acetate:*n*-hexane, 2:8); FT-IR (ATR) in cm^{-1}; 3187 (N−H), 2958 (C−H, Ar), 2917, 2849 (H−C, alkyl asym and sym), 1693 (C=O), 1622 (C=N), 1536, 1464 (C=C), 1169 (C=S); ^{1}H NMR (300 MHz, $CDCl_3$); δ, 12.73 (s, 1H, NH), 9.18 (s, 1H, NH), 8.96 (d, 1H, J = 2.4 Hz, ArH), 8.81 (d, 1H, J = 2.4 Hz, ArH), 8.12 (d, 1H, J = 8.4 Hz, ArH), 7.85 (d, 1H, J = 7.8 Hz, ArH), 7.73 (m, 1H, ArH), 7.59 (m, 1H, ArH), 2.44 (t, 2H, J = 7.5 Hz, CH_2), 1.73 (quin, 2H, J = 7.2 Hz, CH_2), 1.33 (m, 12H, alkyl-H), 0.89 (t, 3H, J = 6.9 Hz, CH_3); ^{13}C NMR (75 MHz, $CDCl_3$); δ, 179.1 (C=O), 174.6 (C=S), 147.3 (C-2, quinolinyl), 146.3, 131.2, 129.5, 129.2, 128.7, 128.0, 127.5, 127.3 (quinolinyl-C), 37.3, 31.8, 29.3, 29.2, 29.1, 29.0, 24.7, 22.6, 14.1 (alkyl-C); Anal. Calcd. for $C_{20}H_{27}N_3OS$: C, 67.19; H, 7.61; N, 11.75; Found: C, 67.15; H, 7.58; N, 11.72.

*2.2.7. N-(Quinolin-3-ylcarbamothioyl)benzamide (**11g**)*

Off-White crystalline (89%); m.p; 118–120 °C; R_f; 0.30 (ethyl acetate:*n*-hexane, 4:6); FT-IR (ATR) in cm^{-1}; 3219 (N−H), 3038 (C−H, Ar), 1667 (C=O), 1605 (C=N), 1511, 1490 (C=C), 1151 (C=S); ^{1}H NMR (300 MHz, $CDCl_3$); δ, 12.69 (s, 1H, NH), 9.17 (s, 1H, NH), 8.93 (d, 1H, J = 2.1 Hz, ArH), 8.68 (d, 1H, J = 2.1 Hz, ArH), 8.22 (d, 2H, J = 7.8 Hz, ArH), 8.05 (d, 1H, J = 8.1 Hz, ArH), 7.83 (d, 1H, J = 8.1 Hz, ArH), 7.73 (m, 1H, ArH), 7.65 (m, 1H, ArH), 7.59 (m, 1H, ArH), 7.54 (m, 2H, ArH); ^{13}C NMR (75 MHz, $CDCl_3$); δ, 178.2 (C=O), 175.1 (C=S), 148.5 (C-2, quinolinyl), 146.2, 133.5, 132.4, 130.8, 129.7, 129.4, 128.8, 128.5, 128.1, 127.8, 127.5, 127.3 (Ar−C); Anal. Calcd. for $C_{17}H_{13}N_3OS$: C, 66.43; H, 4.26; N, 13.67; Found: C, 66.40; H, 4.23; N, 13.65.

*2.2.8. 4-Methyl-N-(quinolin-3-ylcarbamothioyl)benzamide (**11h**)*

Light yellow powder (84%); m.p; 184–186 °C; R_f; 0.25 (ethyl acetate:*n*-hexane, 4:6); FT-IR (ATR) in cm^{-1}; 3300 (N−H), 3050 (C−H, Ar), 2993, 2856 (H−C, alkyl asym and sym), 1670 (C=O), 1579 (C=N), 1523, 1495 (C=C), 1155 (C=S); ^{1}H NMR (300 MHz, $CDCl_3$); δ, 12.33 (s, 1H, NH), 9.09 (s, 1H, NH), 8.89 (d, 1H, J = 2.4 Hz, ArH), 8.70 (d, 1H, J = 2.1 Hz, ArH), 8.22 (d, 2H, J = 8.1 Hz, ArH), 8.09 (d, 1H, J = 8.1 Hz, ArH), 7.83 (d, 1H, J = 8.1 Hz, ArH), 7.64 (m, 1H, ArH), 7.57 (m, 1H, ArH), 7.53 (d, 2H, J = 8.1 Hz, ArH), 2.32 (s, 3H, CH_3); ^{13}C NMR (75 MHz, $CDCl_3$); δ, 177.9 (C=O), 174.1 (C=S), 148.7 (C-2, quinolinyl), 146.2, 141.4, 133.7, 132.3, 130.9, 129.9, 129.2, 128.7, 128.3, 128.0, 127.7, 127.4 (Ar−C), 21.4; Anal. Calcd. for $C_{18}H_{15}N_3OS$: C, 67.27; H, 4.70; N, 13.07; Found: C, 67.24; H, 4.67; N, 13.04.

*2.2.9. 2,4-Dichloro-N-(quinolin-3-ylcarbamothioyl)benzamide (**11i**)*

White powder (84%); m.p; 226–228 °C; R_f; 0.45 (ethyl acetate:*n*-hexane, 4:6); FT-IR (ATR) in cm^{-1}; 3174 (N−H), 3036 (C−H, Ar), 1695 (C=O), 1574 (C=N), 1532, 1493 (C=C), 1165 (C=S); ^{1}H NMR (300 MHz, $CDCl_3$); δ, 12.38 (s, 1H, NH), 9.21 (s, 1H, NH), 8.89 (d, 1H, J = 2.1 Hz, ArH), 8.69 (d, 1H, J = 2.1 Hz, ArH), 8.11 (d, 1H, J = 8.4 Hz, ArH), 7.85 (d, 1H, J = 8.1 Hz, ArH), 7.78 (s, 1H, ArH), 7.64 (m, 1H, ArH), 7.59 (m, 1H, ArH), 7.52 (d, 1H, J = 7.8, ArH), 7.44 (d, 1H, J = 7.8, ArH); ^{13}C NMR (75 MHz, $CDCl_3$); δ, 177.8 (C=O), 174.8 (C=S), 147.6 (C-2, quinolinyl), 146.0, 141.7, 135.7, 133.4, 130.9, 129.9, 129.0, 128.6, 128.2, 128.0, 127.8, 127.2 (Ar−C); Anal. Calcd. for $C_{17}H_{11}C_{l2}N_3OS$: C, 54.27; H, 2.95; N, 11.17; Found: C, 54.24; H, 2.93; N, 11.14.

*2.2.10. 3,5-Dinitro-N-(quinolin-3-ylcarbamothioyl)benzamide (**11j**)*

Light brown (76%); m.p; 188–190 °C; R_f; 0.21 (ethyl acetate:*n*-hexane, 4:6); FT-IR (ATR) in cm^{-1}; 3257 (N−H), 3097 (C−H, Ar), 1668 (C=O), 1626 (C=N), 1538, 1508 (C=C), 1160 (C=S); ^{1}H NMR (300 MHz, $CDCl_3$); δ, 12.23 (s, 1H, NH), 9.20 (s, 1H, NH), 9.10 (s, 1H, ArH), 8.82 (d, 1H, J = 2.4 Hz, ArH), 8.70 (s, 1H, ArH), 8.65 (s, 1H, ArH), 8.62 (d, 1H, J = 2.1 Hz, ArH), 8.21 (d, 1H, J = 7.8, ArH), 8.13 (d, 1H, J = 8.4 Hz, ArH), 7.63 (m, 1H, ArH), 7.59 (m, 1H, ArH); ^{13}C NMR (75 MHz, $CDCl_3$); δ, 176.7 (C=O), 174.7 (C=S), 149.1 (Ar−C), 148.6 (C-2, quinolinyl), 147.2, 146.5, 141.5, 136.7, 133.3, 130.8, 129.7, 128.8, 128.6, 127.8, 125.2 (Ar−C); Anal. Calcd. for C, 51.38; H, 2.79; N, 17.62; Found: C, 51.35; H, 2.76; N, 17.61.

2.3. Mushroom tyrosinase inhibition assay

The mushroom tyrosinase (Sigma Chemical, USA) inhibition assay was performed using our already reported methods [13,20–22]. In detail, 140 μL of phosphate buffer (20 mM, pH 6.8), 20 μL of mushroom tyrosinase (30 U/mL) and 20 μL of the inhibitor solution were placed in the wells of a 96-well microplate. After pre-incubation for 10 min at room temperature, 20 μL of L-DOPA (3,4-dihydroxyphenylalanine, Sigma Chemical, USA) (0.85 mM) was mixed and the assay plate was further incubated at 25 °C for 20 min. Afterward, the absorbance of dopachrome was measured at 475 nm using a microplate reader (OPTI Max, Tunable). Kojic acid was used as a reference inhibitor in this activity and phosphate buffer was used as a negative control. The quantity of inhibition by the test compounds was described as the percentage of concentration necessary to achieve 50% inhibition (IC_{50}). Each concentration was observed in three independent experiments. IC_{50} values were measured by nonlinear regression with GraphPad Prism 5.0.

The % Inhibition of tyrosinase was calculated as following:

$$\text{Inhibition } (\%) = [(B - S)B] \times 100$$

Here, the S and B are the absorbances for the samples and blank.

2.4. Kinetic analysis:

Based on $IC_{50,}$ the most potent compound **11c** for kinetic analysis was selected. Numerous experiments were performed to note the inhibition kinetics of **11c** by following the reported methods [20–22]. The concentrations of inhibitors **11c** were 0.00, 0.0035, 0.007 and 0.014 μM. The concentrations of substrate L-DOPA were between 0.125 and 2 mM in complete kinetic studies. Pre-incubation time and measurement time was the similar as described in the mushroom tyrosinase inhibition activity procedure. Maximal initial velocity was measured from the initial linear area of absorbance for five minutes after mixing of enzyme at a 30 s interval. The inhibition type of the enzyme was assessed by Lineweaver–Burk plots of the inverse of velocities ($1/V$) against the inverse of substrate concentration $1/[L\text{-DOPA}]$ mM^{-1}. The EI dissociation constant *Ki* was measured by the secondary plot of $1/V$ against inhibitors concentrations.

2.5. Free radical scavenging assay

Radical scavenging potential was checked by modifying the known method [23,24] by 2, 2-diphenyl-1 picrylhydrazyl (DPPH) assay. The assay solution composed of 100 μL of DPPH (150 μM), 20 μL of

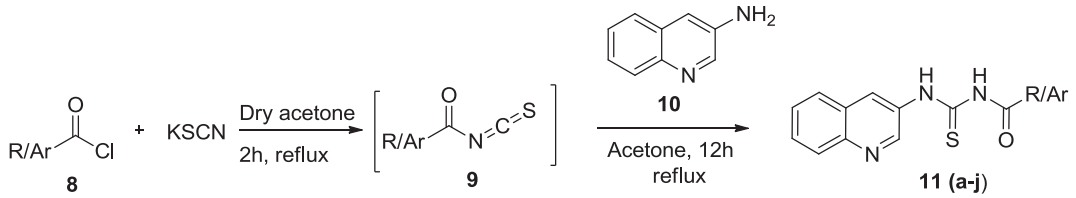

11a; R = propyl **11f**; R = nonyl
11b; R = butyl **11g**; R = phenyl
11c; R = pentyl **11h**; R = 4-Me phenyl
11d; R = hexyl **11i**; R = 2,4-diCl phenyl
11e; R = heptyl **11j**; R = 3,5-dinitrophenyl

Scheme 1. Synthetic route for the quinoline based acyl thioureas **11** (**a-j**).

elevating concentration of sample compounds and the volume was fixed to 200 µL in every well with methyl alcohol. After this, the reaction mixture was incubated at room temperature up to thirty minutes. Ascorbic acid (Vitamin C) was used as a standard inhibitor. The assay measurements were performed by using a microplate reader (OPTI $_{Max}$, Tunable) at wavelength 517 nm. The reaction rates were analyzed, and the percent inhibition caused by the presence of tested inhibitors was calculated. Each concentration was tested in three independent experiments conducted in triplicate.

2.6. Repossession of mushroom tyrosinase structure from PDB

The crystal structure of mushroom tyrosinase (*Agaricus bisporus*) having PDBID: 2Y9X was retrieved form the Protein Data Bank (PDB) (http://www.rcsb.org). This protein structure was minimized by using conjugate gradient algorithm and amber force field in UCSF Chimera 1.10.1 [25]. The stereo-chemical characteristics, Ramachandran graph and values [26] of mushroom tyrosinase were evaluated by Molprobity server [27], while the Ramachandran graph was produced by Discovery Studio 2.1 Client [28]. The protein architecture and statistical percentage values of helices, beta-sheets, coils and turns were retrieved by VADAR 1.8 [29].

2.7. In-silico designing of synthesized compounds

The synthesized compounds **11** (**a-j**) were drawn in ACD/ChemSketch tool and then minimized by visualizing software UCSF Chimera 1.10.1. Molsoft (http://www.molsoft.com/) was used to check the biological properties and drug-likeness of these designed molecules. The number of hydrogen bond acceptors (HBA) and hydrogen bond donors (HBD) were also assessed by PubChem (https://pubchem.ncbi.nlm.nih.gov/). Moreover, all the compounds were endorsed by Lipinski's rule of five (RO5).

2.8. Molecular docking

The prepared ligands **11** (**a-j**) were drawn in ACD/ChemSketch tool and minimized by UCSF Chimera 1.10.1. All the ligands **11** (**a-j**) were sketched in ACD/ChemSketch tool and access in mol format. Furthermore, UCSF Chimera 1.10.1 tool was used to decrease the energy of each ligand separately having default criterion such as steepest descent steps 100 with step size 0.02 (Å), conjugate gradient steps 100 with step size 0.02 (Å) and update interval was fixed at 10. Eventually, Gasteiger charges were added using Dock Prep in ligand structure to get the good structure conformation. Molecular docking test was used for all the ligands towards α-glucosidase by employing PyRx virtual screening tool with Auto Dock VINA Wizard approach. The grid box center values were adjusted as for X = −2.4528, Y = 21.4728 and Z = −31.9954), respectively. The size of grid box was adjusted big enough on biding pocket residues to permit the ligand to move easily in the search space. The default exhaustiveness value = 8 was adjusted in both docking to maximize the analysis of binding conformational. In all docked complexes, the ligands conformational poses were deeply observed to attain excellent docking results. The docked complexes were assessed on lowest binding energy (Kcal/mol) values and structure activity relationship analyses. The graphical depictions of all the docking complexes were performed using Discovery Studio (2.1.0).

3. Results and discussion

3.1. Chemistry

A series of novel acyl thioureas analogues (**11a-j**) were prepared by reacting the potassium thiocyanate with different acid chloride in dry acetone for one hour to afford acyl isothiocyanate (9). The latter was refluxed with a solution of 3-aminoquinoline in dry acetone for 2 h. The crude products were recrystallized with ethanol to furnish in yields shown in Scheme 1.

3.2. Spectroscopic characterization

The synthesized analogues of quinoline based acyl thioureas were characterized by FTIR, NMR and HPLC-MS. Three characteristics types of protons resulted in distinct signals in ^{1}H NMR spectrum. The signals for two N−H protons appeared as singlets at 12.74 ppm and 9.36 ppm. These signals are deshielded owing to inter- and intramolecular hydrogen bonding indicating the presence of C═S in neighbor of N−H. The aromatic protons gave rise to signals in region of 7–9 ppm while the signals in the region of 0.8–2.5 ppm indicated the alkyl protons. In ^{13}C NMR spectrum, the signals appeared at 179.2 ppm and 174.8 ppm were assigned to the C═O and C═S, respectively. The aromatic carbons resulted in the signals at 125–147 ppm with weak intense signals for ipso carbons. Alkyl carbons gave the signals in the range of 13–40 ppm. In FTIR, the broad absorption near 3200 cm^{-1} was assignable to N−H of thiourea. The aromatic C−H stretch caused the absorption band in the region of 3200–3050 cm^{-1}. The absorption band for C═O bond was present in the range of 1700–1600 cm^{-1}.

3.3. Mushroom tyrosinase inhibition assay

The synthesized compounds **11** (**a-j**) were screened to validate their significance as tyrosinase enzyme inhibitors. The standard compound used for the screening was Kojic acid and results of evaluation as half maximal inhibitory concentration (IC_{50}) are summarized in Table 1. Interestingly, all synthesized compounds showed convincing inhibition potential towards mushroom tyrosinase. Moreover, all compounds exhibited better inhibition potential comparative to Kojic acid and the compound **11c** (IC_{50} = 0.0070 ± 0.0098) was dominant tyrosinase inhibitors as compared to other analogues in the series.

The nature of functionalities around the acyl thiourea moiety greatly affected the tyrosinase inhibition activity. The sterically

Table 1
IC_{50} values of compounds **11** (**a-j**) values were calculated by nonlinear regression using GraphPad Prism 5.0.

Compound	Tyrosinase activity IC_{50} ± SEM (μM)
11a	1.9737 ± 0.6541
11b	0.4196 ± 0.0748
11c	0.0070 ± 0.0098
11d	0.1105 ± 0.0995
11e	0.1149 ± 0.0014
11f	0.2685 ± 0.0065
11g	0.0148 ± 0.0011
11h	0.1275 ± 0.8745
11i	0.7656 ± 0.0254
11j	0.1099 ± 0.0113
Kojic acid	16.8320 ± 0.0621

SEM = Standard error of the mean.

hindered substituents like long alkyl chains in the compounds resulted in diminishing the inhibitory effect. The compound **11c**, containing moderate alkyl chain, thiourea and quinoline moiety, interact strongly and occupy the whole pocket of receptor. The compounds **11a** exhibited comparatively least inhibitory activity due to small size, it poorly interacted with enzyme and unable to occupy the pocket of receptor. The compound **11 g** observed as second potent inhibitor due to the presence phenyl ring instead of long alkyl chain. However, the substituent on the phenyl ring decreased the inhibitory effect due to increased steric hindrance.

3.4. Kinetic analysis

On the basis of results, the most potent compound **11c** was selected to determine its inhibition type and inhibition constant on tyrosinase. The potential of the synthesized compounds to impede free enzyme and enzyme substrate complex was measured in term of EI and ESI constants respectively. The kinetic studies of the enzyme by the Lineweaver-Burk plot of 1/V versus 1/[S] in the presence of different compounds concentrations gave a series of straight lines (Fig. 2a). The results indicated that the compound **11c** intersected within the second quadrant. The analysis revealed that V_{max} decreased to new increasing doses of inhibitors, on the other hand, K_m remains unchanged. This response indicates that compound **11c** inhibits the tyrosinase non-competitively to make enzyme-inhibitor complex. Secondary plot of slope versus the concentration of compounds exhibited enzyme inhibitor dissociation constant (K*i*) (Fig. 2b). The results of kinetic analysis are presented in the Table 2.

Table 2
Kinetic parameter.

Concentration (μM)	V_{max} (ΔA/Sec)	Km (mM)	Type of inhibition	Ki (μM)
0.00	7.75758E-06	0.303	Non-Competitive	0.0087
0.0035	3.33333E-06	0.303		
0.007	3.04659E-06	0.303		
0.014	1.78788E-06	0.303		

V_{max} = Reaction velocity, Km = Michaelis-Menten constant, Ki = EI dissociation constant.

3.5. Free radical scavenging

The synthesized series of the compounds **11** (**a-j**) were assessed for 2,2-Diphenyl-1-(2,4,6-trinitrophenyl)hydrazyl (DPPH) free radical scavenging ability using vitamin C as reference drug. The radical DPPH can scavenge by compounds which donate proton and forming the reduced DPPH [30]. The scavenging potency of compounds **11g** and **11i** was 62 and 82% respectively, while the other compounds did not exhibit scavenging potential. The scavenging potency was related to proton donating ability of the compounds **11g** and **11i** containing phenyl and quinolinyl rings. The compound **11a** exhibited least scavenging activity which can be associated with poor proton donating ability (see Fig. 3).

3.6. Mushroom tyrosinase structural assessment

Mushroom tyrosinase is an enzyme containing copper atoms and consists of 391 residues [31]. The complete structure analysis of target protein showed that, it contains 39% *α*-helices, 14% *β*-sheets and 46% coils. Its resolution (2.78 Å), R-value (0.238) and unit cell crystal

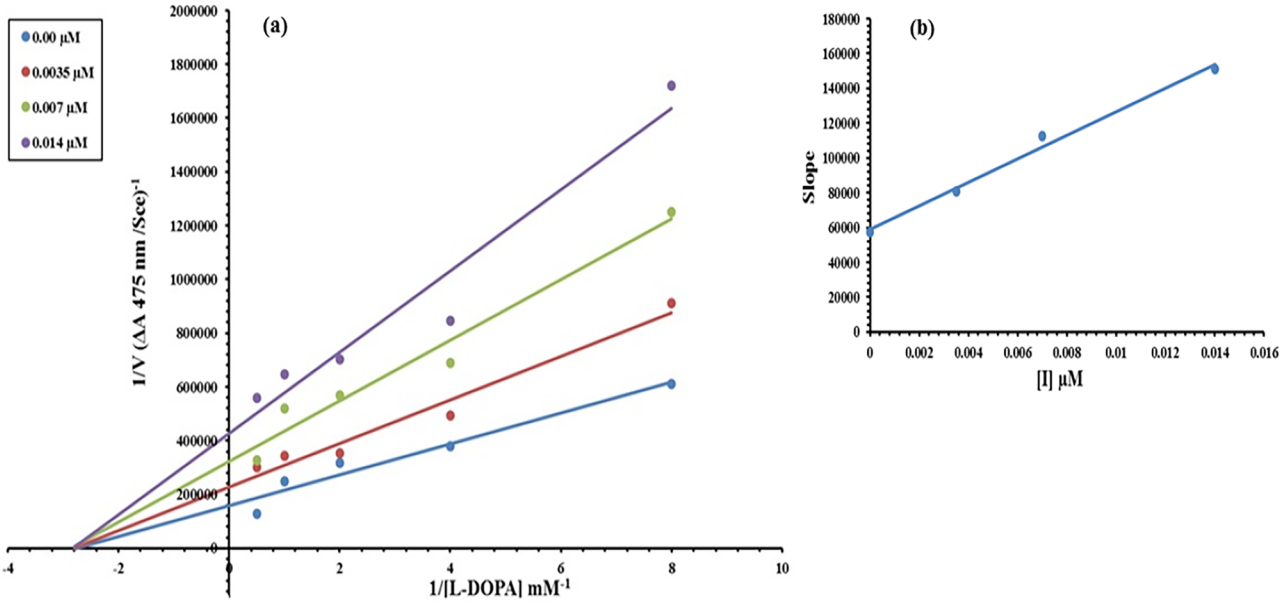

Fig. 2. Lineweaver–Burk plots for tyrosinase inhibition with Compound **11c**. **(a)** Concentrations of **11c** were 0.00, 0.0035, 0.007 and 0.014 μM, respectively. The concentrations of substrate *L*-DOPA were 0.125, 0.25, 0.5, 1 and 2 mM, respectively. **(b)** The insets reveal the plot of the slope against inhibitor **11c** concentrations to find inhibition constant. The lines were sketched with linear least squares fit.

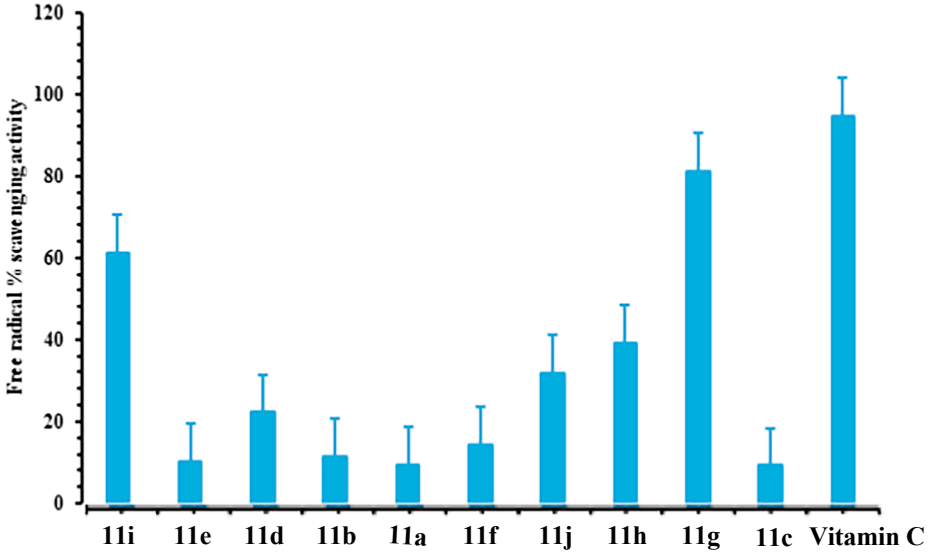

Fig. 3. Free radical % scavenging potential of the synthesized compounds **11** (**a-j**), values are given as mean ± SEM. The concentration of each compound was 100 µg/mL.

dimensions such as coordinates angles and length was confirmed by X-ray diffraction. The Ramachandran plots and values showed that 95.90% of protein residues were lie in favored region and 100.0% residues were exist in allowed region. The Ramachandran graph values exhibited the good accuracy of phi (φ) and psi (ψ) angles between the receptor's coordinates and many residues were jumped in acceptable region.

3.7. Chemo-informatics properties and Lipinski rule (RO5) evaluation of ligands

The designed ligands were analyzed computationally to predict their biological properties and RO5 validity (Table 3). The predicted chemo-informatics properties were Mol Wt (g/mol) HBD, HBA, Log*P*, polar surface area (PSA), molar volume and drug likeness score of ligand molecules. Literature study confirmed that the standard values for Mol Wt (≤500 g/mol) [32]. The ligands predicted results showed that compounds possessed good Mol Wt as compared to standard value. Research data showed poor permeation is more probable to be observed when the HBA and HBD are increased from 10 and 5 respectively, [33]. The chemo-informatics analysis vindicated that all the designed ligands have < 10 HBA and < 5 HBD. Moreover, their log*P* values were also similar to standard value except the **11f** which exhibited higher than 5. All the synthetic compounds fully obeyed the RO5. However, plenty of examples is available for RO5 violation amongst the present drugs [34,35]. Furthermore, the polar surface area (PSA) or total polar surface area is also known as significant parameter for the development of drug. Commonly, the PSA parameter is used for drug's optimization ability to permeate cells. The research data revealed the standard value of PSA (< 89 A^2) [36]. Our predicted results indicated that compounds possessed similar results.

Table 3
Chemo-informatics analysis of compounds **11** (**a-j**).

Ligands	Mol. Wt (g/mol)	No. HBA	No. HBD	Mol. Log*p* (mg/L)	PSA (A^2)	Mol. Vol (A^3)
11a	273	3	2	2.77	42	271
11b	287	3	2	3.25	42	289
11c	301	3	2	3.73	42	307
11d	315	3	2	4.21	42	325
11e	329	3	2	4.70	42	343
11f	357	3	2	5.66	42	379
11g	307	3	2	3.22	42	289
11h	321	3	2	3.63	42	310
11i	375	3	2	4.53	42	322
11j	397	7	2	2.68	118	341

Abbreviations: HBA = Number of hydrogen bond acceptor, HBD = Number of hydrogen bond donor, Log*P* = lipophilicity of partition coefficient, LogS = lipophilicity of water, PSA = polar surface area.

3.8. Molecular docking analyses

Molecular docking analyses is an efficient approach to examine the binding conformation of ligands towards target protein [37,38]. The docked complexes of compounds **11a-j** versus tyrosinase were studied on the basis of minimum binding energy values (kcal/mol) and hydrogen/hydrophobic interaction pattern. The results revealed that all the ligands (**11a-j**) showed good docking energy values and exhibited their interaction inside active region of target protein (Table 4). The docking energy values were determined by using Eq. (1) for all the ligands.

$$\Delta G\ \ binding = \Delta Ggauss + \Delta Grepulsion + \Delta Ghbond + \Delta Ghydrophobic + \Delta Gtors \quad (1)$$

Here, ΔG gauss: term for distribution of two gaussian functions, ΔGrepulsion: square of the distance if nearer than a threshold value, ΔGhbond: ramp function - also used for interactions with metal ions, ΔGhydrophobic: ramp function, ΔGtors: proportional to the number of rotatable bonds. In docking energy results, compounds selected as best

Table 4
Docking energy values of all ligands.

Mushroom tyrosinase Docking complexes	Binding Affinity (Kcal/mol)
11a	−6.8
11b	−6.4
11c	−7.2
11d	−6.4
11e	−6.5
11f	−6.5
11g	−7.0
11h	−7.4
11i	−7.2
11j	−7.4

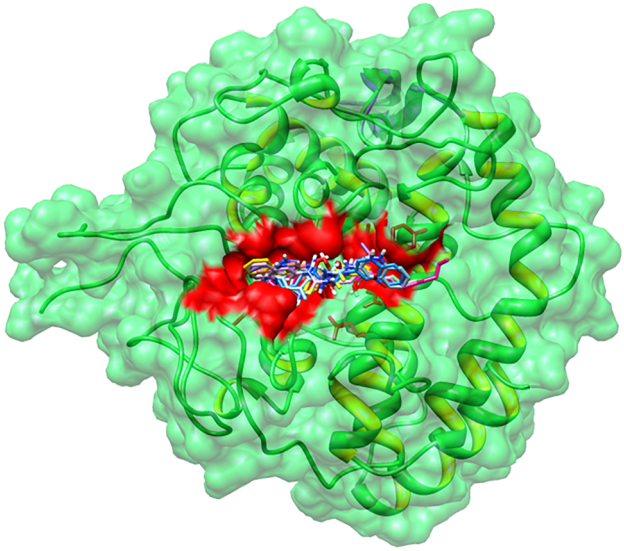

Fig. 4. Binding of ligands within active region off target protein. The receptor molecule is painted in light green color in ribbon and surface format. However, all ligands are justified in different colors.

having greater than 2.5 kcal/mol energy value difference compared to other compounds. The standard error for Autodock is reported as 2.5 kcal/mol (http://autodock.scripps.edu/) [39]. Present docking results justified that the energy value difference among all docking complexes were lower than standard error value. Therefore, based on the basis of both *in vitro* and *in silico* docking energy results, **11c** was ranked as best ligand which showed good inhibitory potential against targeted enzyme as compared all other derivatives. Large fluctuations in energy were not observed because all the compounds contain same nucleus. Most of the ligands possess efficient energy values.

3.9. Binding pocket and ligands binding conformations

The binding pocket analysis exhibited that all ligands were limited to the active region of target protein nearby copper metal. All the docked structures were superimposed to notice the binding configuration of the ligands in the active section of mushroom tyrosinase. Results showed that the synthesized ligands were bind in the binding pocket having at least similar conformational pattern. All ligands showed little deviation around their axis in configuration shape. The quinoline moiety in most of the compounds showed their binding pattern in the opening gate of binding pocket. Whereas, the presence of different incorporated functional moiety showed their attachment inside the binding pocket near the copper metal. Most of ligands were binds at same position which justify our docking results reliability (Fig. 4). Fig. 5 showed the binding pattern of most active ligand (**11c**) in the active region of the target protein. The **11c**-docking complex showed that incorporated functional group showed its penetration within the binding pocket and may have potential. This incorporation may result in suitable configuration and conformation to ligands to be fitted in the binding pocket of mushroom tyrosinase.

3.10. Hydrogen and hydrophobic binding interaction between *11c* and target protein

The binding interaction exhibited that **11c** directly binds with active region residues of enzyme mushroom tyrosinase. Binding analysis showed that **11c** forms single hydrogen bond with amino acid His244 and three hydrophobic interaction with Glu256, His263 and Val28, respectively. The sulfur atom of thiocarbonyl group forms a hydrogen bond with His244 having good binding distance 2.74 Å. Similarly, nitrogen atom of same group was involved with Glu256 by hydrophobic interaction with bond length 4.86 Å. The incorporated non-aliphatic chain from two hydrophobic bonds with Val283 and His263 (π-alkyl) with bond distances 4.76 and 4.03 Å, respectively. The aromatic His263 is metal bounded residue which may have significant role in activation and functionality of tyrosinase. Our incorporated functional moiety directly indulges with functional residues of target protein and showed strong correlation with *in vitro* results. Literature study also vindicated that these binding pocket residues are important in downstream signaling paths [13,20,31]. The graphical representation of **11c** docking complex is given in Fig. 6 and all other complexes in supplementary data.

4. Conclusions

The quinolinyl based acyl thiourea derivatives (**11a-j**) containing alkyl and aryl groups were prepared and characterized by FT-IR, ^{1}H

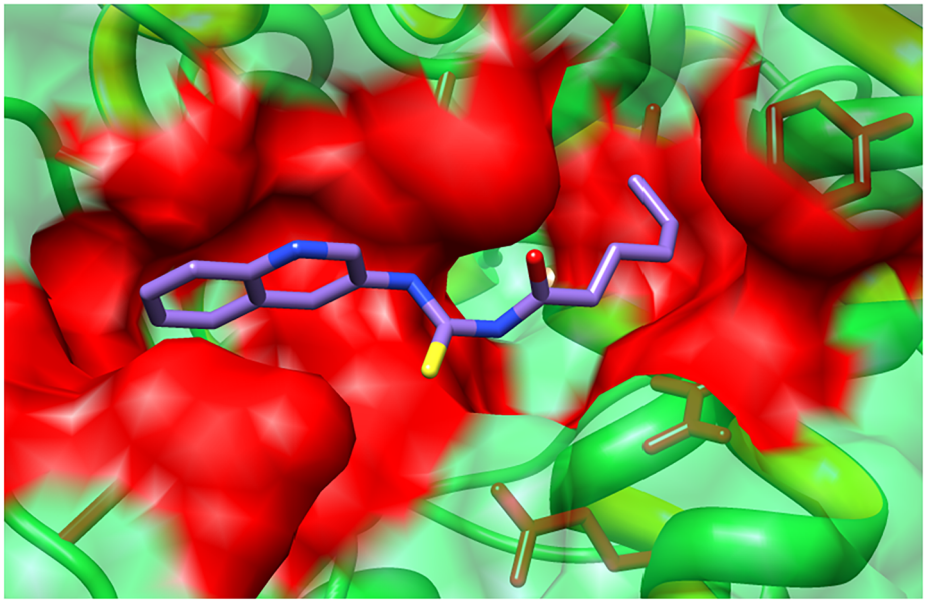

Fig. 5. Binding conformation of **11c** in the active region of target protein.

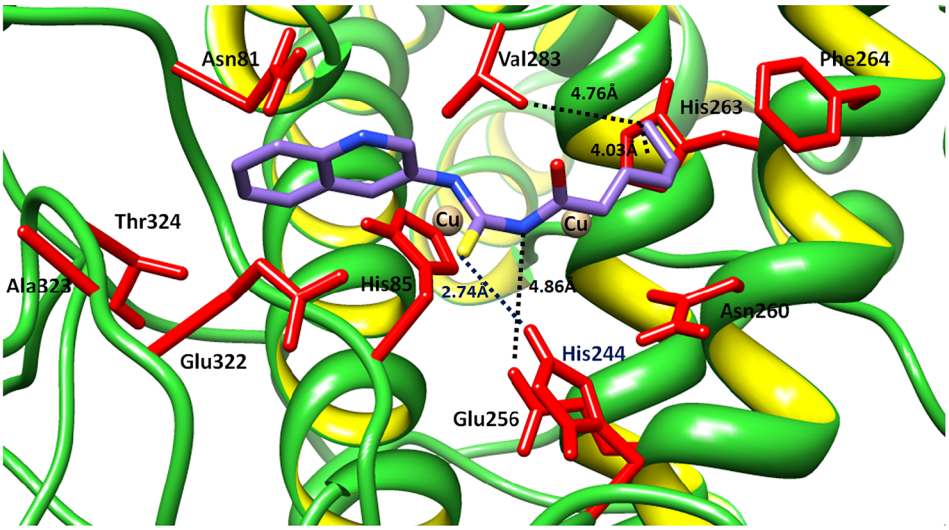

Fig. 6. Molecular docking interaction of compound **11c** with receptor molecule. The protein structure is demonstrated in green color in ribbon format while ligand is represented in purple color and their functional groups such as amino, sulfur and oxygen are presented in red, blue and yellow colors, respectively. The residues involved in hydrogen bonds are labeled in blue while hydrophobic interacted residues are painted in black colors, respectively. Blue and black dotted lines with length mentioned in angstrom (Å) are presented for hydrogen and hydrophobic bond distances. Two copper ions are represented in light maroon circles.

NMR, ^{13}C NMR and HPLC-MS. Mushroom tyrosinase inhibition assay, kinetic and molecular docking analysis were performed for all the compounds. The compound *N*-(quinolin-3-ylcarbamothioyl)hexanamide (**11c**) exhibited higher tyrosinase inhibition activity ((IC_{50} = 0.0070 ± 0.0098 μM) compared to other analogues. Kinetic analysis revealed that the derivative (**11c**) was non-competitive inhibitor with Ki value of 0.0087 μM. The molecular docking showed that the compound (**11C**) possesses efficient binding affinity (−7.2 kcal/mol) with protein (PDBID: 2Y9X). The presence of quinolinyl and alkyl group in thiourea play significant role in tyrosinase inhibition effect. The compound **11c** could be identified as potent tyrosinase inhibitor that might be promising lead in medicine, cosmetics and food industry.

Appendix A. Supplementary data

Supplementary data to this article can be found online at https://doi.org/10.1016/j.bioorg.2019.103063.

References

[1] A. Saeed, R. Qamar, T.A. Fattah, U. Flörke, M.F. Erben, Recent developments in chemistry, coordination, structure and biological aspects of 1-(acyl/aroyl)-3-(substituted) thioureas, Res. Chem. Intermed. 43 (5) (2017) 3053–3093.
[2] J. Małecki, J. Nycz, Ruthenium (II) hydridecarbonyl complex with *N*, N′-bis-(2-pyridyl) thiourea as co-ligand, Polyhedron 55 (2013) 49–56.
[3] S. Hasan, N.A. Hamedan, H.M. Zaki, Application of P-dimethylaminobenzaldehyde benzoylthiourea as a colorimetric chemosensor for detection of Cu2+ in aqueous solution, Int. J. Chem. Eng. Appl. 8 (1) (2017) 22.
[4] L. Colina-Vegas, L. Luna-Dulcey, A.M. Plutín, E.E. Castellano, M.R. Cominetti, A.A. Batista, Half sandwich Ru (II)-acylthiourea complexes: DNA/HSA-binding, anti-migration and cell death in a human breast tumor cell line, Dalton Trans. 46 (38) (2017) 12865–12875.
[5] Z. Ali, N.E. Richey, D.C. Bock, K.A. Abboud, J. Akhtar, M. Sher, L. McElwee-White, *N*, N-Disubstituted-N′-acylthioureas as modular ligands for deposition of transition metal sulfides, Dalton Trans. 47 (8) (2018) 2719–2726.
[6] S. Manjula, N.M. Noolvi, K.V. Parihar, S.M. Reddy, V. Ramani, A.K. Gadad, G. Singh, N.G. Kutty, C.M. Rao, Synthesis and antitumor activity of optically active thiourea and their 2-aminobenzothiazole derivatives: a novel class of anticancer agents, Eur. J. Med. Chem. 44 (7) (2009) 2923–2929.
[7] A. Bielenica, E. Kędzierska, M. Koliński, S. Kmiecik, A. Koliński, F. Fiorino, B. Severino, E. Magli, A. Corvino, I. Rossi, 5-HT 2 receptor affinity, docking studies and pharmacological evaluation of a series of 1,3-disubstituted thiourea derivatives, Eur. J. Med. Chem. 116 (2016) 173–186.
[8] S. Saeed, N. Rashid, P.G. Jones, M. Ali, R. Hussain, Synthesis, characterization and biological evaluation of some thiourea derivatives bearing benzothiazole moiety as potential antimicrobial and anticancer agents, Eur. J. Med. Chem. 45 (4) (2010) 1323–1331.
[9] Z. Zhong, R. Xing, S. Liu, L. Wang, S. Cai, P. Li, Synthesis of acyl thiourea derivatives of chitosan and their antimicrobial activities in vitro, Carbohydr. Res. 343 (3) (2008) 566–570.
[10] K.M. Khan, F. Naz, M. Taha, A. Khan, S. Perveen, M. Choudhary, W. Voelter, Synthesis and in vitro urease inhibitory activity of *N*, N′-disubstituted thioureas, Eur. J. Med. Chem. 74 (2014) 314–323.
[11] X. Xu, X. Qian, Z. Li, Q. Huang, G. Chen, Synthesis and insecticidal activity of new substituted *N*-aryl-*N*′-benzoylthiourea compounds, J. Fluorine Chem. 121 (1) (2003) 51–54.
[12] S. Xue, L. Duan, S. Ke, L. Jia, Synthesis, crystal structure and herbicidal activity of 1-benzoyl-3-(4, 6-disubstituted pyrimidine-2yl)-thiourea derivatives, Chem. Mag. 5 (2003) 67–70.
[13] F.A. Larik, A. Saeed, P.A. Channar, U. Muqadar, Q. Abbas, M. Hassan, S.-Y. Seo, M. Bolte, Design, synthesis, kinetic mechanism and molecular docking studies of novel 1-pentanoyl-3-arylthioureas as inhibitors of mushroom tyrosinase and free radical scavengers, Eur. J. Med. Chem. 141 (2017) 273–281.
[14] K.-K. Song, H. Huang, P. Han, C.-L. Zhang, Y. Shi, Q.-X. Chen, Inhibitory effects of cis-and trans-isomers of 3, 5-dihydroxystilbene on the activity of mushroom tyrosinase, Biochem. Biophys. Res. Commun. 342 (4) (2006) 1147–1151.
[15] Q.-X. Chen, X.-D. Liu, H. Huang, Inactivation kinetics of mushroom tyrosinase in the dimethyl sulfoxide solution, Biochemistry (Moscow) 68 (6) (2003) 644–649.
[16] W.-C. Chen, T.-S. Tseng, N.-W. Hsiao, Y.-L. Lin, Z.-H. Wen, C.-C. Tsai, Y.-C. Lee, H.-H. Lin, K.-C. Tsai, Discovery of highly potent tyrosinase inhibitor, T1, with significant anti-melanogenesis ability by zebrafish in vivo assay and computational molecular modeling, Sci. Rep. 5 (2015) 7995.
[17] G.C. Priestley, Molecular Aspects of Dermatology vol. 3, Wiley, 1993.
[18] T. Eicher, S. Hauptmann, The Chemistry of Heterocycles, second ed., WileyVCH, Weinheim, 2003, pp. 316–336.
[19] J.K. Baird, K.H. Rieckmann, Can primaquine therapy for vivax malaria be improved? Trends Parasitol. 19 (3) (2003) 115–120.
[20] Q. Abbas, Z. Ashraf, M. Hassan, H. Nadeem, M. Latif, S. Afzal, S.-Y. Seo, Development of highly potent melanogenesis inhibitor by in vitro, in vivo and computational studies, Drug Des. Develop. Therapy 11 (2017) 2029.
[21] A. Saeed, P.A. Mahesar, P.A. Channar, Q. Abbas, F.A. Larik, M. Hassan, H. Raza, S.-Y. Seo, Synthesis, molecular docking studies of coumarinyl-pyrazolinyl substituted thiazoles as non-competitive inhibitors of mushroom tyrosinase, Bioorg. Chem. 74 (2017) 187–196.
[22] Q. Abbas, H. Raza, M. Hassan, A.R. Phull, S.J. Kim, S.Y. Seo, Acetazolamide inhibits the level of tyrosinase and melanin: an enzyme kinetic, in vitro, in vivo, and in silico studies, Chem. Biodivers. 14 (9) (2017) e1700117.
[23] C.V.K. Reddy, D. Sreeramulu, M. Raghunath, Antioxidant activity of fresh and dry fruits commonly consumed in India, Food Res. Int. 43 (1) (2010) 285–288.
[24] Z. Ashraf, M. Rafiq, S.-Y. Seo, M.M. Babar, Synthesis, kinetic mechanism and docking studies of vanillin derivatives as inhibitors of mushroom tyrosinase, Bioorg. Med. Chem. 23 (17) (2015) 5870–5880.
[25] E.F. Pettersen, T.D. Goddard, C.C. Huang, G.S. Couch, D.M. Greenblatt, E.C. Meng, T.E. Ferrin, UCSF Chimera—a visualization system for exploratory research and analysis, J. Comput. Chem. 25 (13) (2004) 1605–1612.
[26] S.C. Lovell, I.W. Davis, W.B. Arendall III, P.I. De Bakker, J.M. Word, M.G. Prisant, J.S. Richardson, D.C. Richardson, Structure validation by Cα geometry: ϕ, ψ and Cβ deviation, Proteins Struct. Funct. Bioinf. 50 (3) (2003) 437–450.
[27] V.B. Chen, W.B. Arendall, J.J. Headd, D.A. Keedy, R.M. Immormino, G.J. Kapral, L.W. Murray, J.S. Richardson, D.C. Richardson, MolProbity: all-atom structure validation for macromolecular crystallography, Acta Crystallogr. Sect. D: Biol. Crystallogr. 66 (1) (2010) 12–21.
[28] D. Studio, Discovery."version 2.1.", Accelrys: San Diego, CA, 2008.
[29] L. Willard, A. Ranjan, H. Zhang, H. Monzavi, R.F. Boyko, B.D. Sykes, D.S. Wishart, VADAR: a web server for quantitative evaluation of protein structure quality, Nucleic Acids Res. 31 (13) (2003) 3316–3319.
[30] M. Mon, S. Maw, Z. Oo, Quantitative determination of free radical scavenging activity and anti-tumor activity of some Myanmar herbal plants, World Acad. Sci. Eng. Technol 75 (2011) 524–530.
[31] Z. Ashraf, M. Rafiq, H. Nadeem, M. Hassan, S. Afzal, M. Waseem, K. Afzal, J. Latip, Carvacrol derivatives as mushroom tyrosinase inhibitors; synthesis, kinetics mechanism and molecular docking studies, PloS One 12 (5) (2017) e0178069.

[32] R. Kadam, N. Roy, Recent trends in drug-likeness prediction: A comprehensive review of In silico methods, Indian J. Pharm. Sci. 69 (5) (2007) 609.
[33] M.A. Bakht, M.S. Yar, S.G. Abdel-Hamid, S.I. Al Qasoumi, A. Samad, Molecular properties prediction, synthesis and antimicrobial activity of some newer oxadiazole derivatives, Eur. J. Med. Chem. 45 (12) (2010) 5862–5869.
[34] S. Tian, J. Wang, Y. Li, D. Li, L. Xu, T. Hou, The application of in silico drug-likeness predictions in pharmaceutical research, Adv. Drug Deliv. Rev. 86 (2015) 2–10.
[35] P.B. Jadhav, A.R. Yadav, M.G. Gore, Concept of drug likeness in pharmaceutical research, Int. J. Pharm. Biol. Sci 6 (2015) 142–154.
[36] A.K. Ghose, T. Herbertz, R.L. Hudkins, B.D. Dorsey, J.P. Mallamo, Knowledge-based, central nervous system (CNS) lead selection and lead optimization for CNS drug discovery, ACS Chem. Neurosci. 3 (1) (2011) 50–68.
[37] M. Hassan, Z. Ashraf, Q. Abbas, H. Raza, S.-Y. Seo, Exploration of novel human tyrosinase inhibitors by molecular modeling, docking and simulation studies, Interdis. Sci.: Comput. Life Sci. 10 (1) (2018) 68–80.
[38] M. Hassan, Q. Abbas, Z. Ashraf, A.A. Moustafa, S.-Y. Seo, Pharmacoinformatics exploration of polyphenol oxidases leading to novel inhibitors by virtual screening and molecular dynamic simulation study, Comput. Biol. Chem. 68 (2017) 131–142.
[39] P.A. Channar, A. Saeed, F. Albericio, F.A. Larik, Q. Abbas, M. Hassan, H. Raza, S.-Y. Seo, Sulfonamide-linked ciprofloxacin, sulfadiazine and amantadine derivatives as a novel class of inhibitors of jack bean urease; synthesis, kinetic mechanism and molecular docking, Molecules 22 (8) (2017) 1352.